POLITECNICO DI TORINO
Repository ISTITUZIONALE

Efficient agricultural practices in Africa reduce crop water footprint despite climate change, but rely on blue water resources

Original
Efficient agricultural practices in Africa reduce crop water footprint despite climate change, but rely on blue water resources / Giordano, V., Tuninetti, M., Laio, F.. - In: COMMUNICATIONS EARTH & ENVIRONMENT. - ISSN 2662-4435. - 4:1(2023). [10.1038/s43247-023-01125-5]

Availability:
This version is available at: 11583/2996583 since: 2025-01-14T14:20:19Z

Publisher:
Nature Publishing Group

Published
DOI:10.1038/s43247-023-01125-5

Terms of use:

This article is made available under terms and conditions as specified in the corresponding bibliographic description in the repository

Publisher copyright

(Article begins on next page)

28 November 2026

communications earth & environment

ARTICLE

https://doi.org/10.1038/s43247-023-01125-5 OPEN

Efficient agricultural practices in Africa reduce crop water footprint despite climate change, but rely on blue water resources

Vittorio Giordano [1]✉, Marta Tuninetti [1] & Francesco Laio[1]

Alarming projections of climate change, decline in crop yields, and increased food demand constitute daunting threats to African food production and sustainable water management. Here, we map this complex water-food nexus by combining gridded climate data and process-based crop modelling to quantify scenarios of crop water footprint under Representative Concentration Pathway 2.6 and Representative Concentration Pathway 6.0 for time horizons 2040, 2070 and 2100. We show that high-input agricultural management coupled with the expansion of irrigation infrastructure could generate an average reduction of water use intensity up to 64% for staple crops, but only 5% for cash crops, by 2040. Notwithstanding the positive effect of intensification, between 82 Km^3 (2040) and 102 Km^3 (2100) of additional blue water will be required to sustain the increased yields. Our scenarios are suited for identifying locations where crops are subject to high climate impacts and where crop production shows trade-offs between high-input management and irrigation demand.

[1] Department of Environment, Land, and Infrastructure Engineering, Politecnico di Torino, Turin, Italy. ✉email: vittorio.giordano@polito.it

Warmer mean and extreme temperatures, growing atmospheric CO_2 concentrations, altered precipitation regimes, and drought patterns affect agricultural production worldwide[1,2]. At the same time crop yields are expected to decrease under future climate conditions[3], with the largest adverse impacts expected at low latitudes[1,4,5]. In parallel, the world is experiencing rising demand for crop production, which stems from increasing affluence and consumption habits, changing living standards and biofuel proliferation[6]. Meeting such demand is a formidable and multi-faceted challenge[6,7], even more relevant considering the COVID-19 pandemic and the war in Ukraine impacts on food-security worldwide[8,9]. Recent studies have suggested multiple strategies, including sustainable intensification, which show large potential for meeting demand challenges and mitigating climate change, without further encroachment on natural ecosystems[4,6,10,11]. Although promising, such solutions would necessitate major investments in modern technology and large additional inputs of water and fertilizers[12].

The African population faces the world's highest malnutrition[9,13], severe water scarcity and poverty[14,15], while anthropogenic climate change is expected to further compromise water availability and food security on the continent in the coming decades[16,17]. Insufficient food supply is still one of the main causes for hunger on the continent[18]; therefore, researchers and policy makers have called for a boost in crop yields through the enhancement of agricultural production practices[19]. However, it is not yet clear to what extent this might exacerbate the impacts on water resources and how climate change may limit its effectiveness[11,20]. Here, we fill this crucial gap for the African continent by developing spatially explicit future scenarios of crop water footprint to explore the implications of unprecedented crop yield growth under a changing climate on water resources. We assume crop productivity to increase up to the maximum attainable yield by 2040, as a result of an intensive and high-input agricultural management projected on the continent[21,22] and of the expansion of irrigation infrastructure over all rainfed harvested areas[23]. The crop water footprint (CWF) is a useful indicator to analyse the water-food nexus[24–26], since it provides a framework to examine the linkages between human consumption and the direct and indirect appropriation of global freshwater[27]. Most of the studies so far have explored future global CWF scenarios[28] or process-based future projections of CWF responses to climate change at country or basin level[29,30], while few have computed sub-national and high-resolution scenarios of CWF[31–33]. We advance this research field by designing spatially explicit crop water footprint scenarios at 5 arc min resolution (~ 10 km resolution at the equator), under RCP 2.6 and RCP 6.0, for the time horizons 2040, 2070, and 2100, while using 2010 as the reference year[34]. Through the model WaterCROP[24], we combine future projections of crop evapotranspiration and yield of twelve crops, with a holistic approach which integrates emissions pathways with improved agricultural management conditions and irrigated areas expansion. From 2040 onward we attribute to all simulations advanced agricultural management practices with high inputs levels, which allow yields to grow up to their maximum attainable value. Thus, we describe an agricultural system which is mainly market oriented, fully mechanized and which employs optimal irrigation, high yielding varieties, nutrients and chemical pest, disease and weed control application. This assumption has been constrained with time-independent harvested areas, constant at year 2010 extension, in order to simulate a pathway of agricultural intensification over the continent, which we address as Hard-intensification pathway, coherent with the shared socio-economic pathway (SSP) SSP 5 - Taking The Highway[35]. The impressive yield growth and the fixed cropland extension constitute highly optimistic assumptions, which we discuss by comparing our results with current trends of extensification projected to 2040; thus defining an Extensification pathway, coherent with SSP 2 - Middle of The Road[35].

Results and discussion

Water footprint spatial distribution and the signature of climate change. We develop one baseline (2010) and three future scenarios (for the time horizons: 2040, 2070, 2100) of unitary (uWF) and total (WF) crop water footprint, each resulting from a 30-years average evaluated from annual-based estimates of crop actual evapotranspiration (ET_a) and yield (see "Materials and Methods"). While uWF measures the intensity of crop water use, the WF measures the total volume of water used for crop production[36]. We observe predominantly increasing trends among the WF volumes of the twelve crops analysed - barley, cassava, cotton, groundnut, maize, millet, rice, sorghum, soybean, sugarcane, wheat and yam (Table 1) - chosen among the major food crops grown in Africa, including two of the principal cash-crops (cotton and sugarcane). Figure 1 shows the green and blue WF distribution on Africa's harvested areas in 2010 - respectively, the contributions of soil moisture (green water) and irrigation (blue water) to the crop water demand (panels a, c). The highest concentration of green water use is localized along the Sahel strip, with Nigeria recording the highest green WF in 2010 ($1.22 \cdot 10^{11}$ m^3; see Supplementary Fig. 4 for country level green WF values), followed by Niger and Sudan. The difference between rainfed harvested areas and irrigated land extension is striking, the locations where water resources are exploited for irrigation purposes are predominantly located along the Nile river and in South Africa, and Egypt is the country with the highest blue WF in 2010 ($1.76 \cdot 10^{10}$ m^3; see Supplementary Fig. 5 for country level blue WF values). Panel b shows the change in green WF in 2040 for RCP6.0, with respect to 2010 (refer to Supplementary Fig. 1 for RCP2.6). This variation is predominantly driven by ET_a and precipitation (P) projections and intensifies in 2070 and 2100 (Supplementary Figs. 2, 3), allowing to attribute the WF evolution to future changes of Earth's climate. The countries bordering the Gulf of Guinea exhibit widespread positive change in green WF, with Equatorial Guinea recording the highest positive average variation of (+7.14%). Rising temperature and crop potential evapotranspiration (ET_c) drive increasing green ET_a where soil moisture availability can sustain this higher demand of green water, such as in the equatorial zone. On the other hand, in the north of the continent and in the Horn of Africa negative changes of green WF can be observed. Here crops respond to rising temperatures with

Table 1 List of the crops included in the study.

Crop	Production [kcal capita^{-1} day^{-1}]	Harvested Area [ha]
Barley	0.89%	1.43%
Cassava	9.01%	7.88%
Cotton	0.00%	1.76%
Groundnut	1.78%	5.92%
Maize	14.81%	14.48%
Millet	2.24%	6.81%
Rice	9.24%	5.91%
Sorghum	4.68%	9.64%
Soybean	0.15%	0.90%
Sugarcane	0.15%	0.55%
Wheat	14.42%	3.37%
Yam	3.21%	3.03%
Total	60.60%	61.67%

For each crop, the table shows the percentage of crop production and harvested area in 2019.

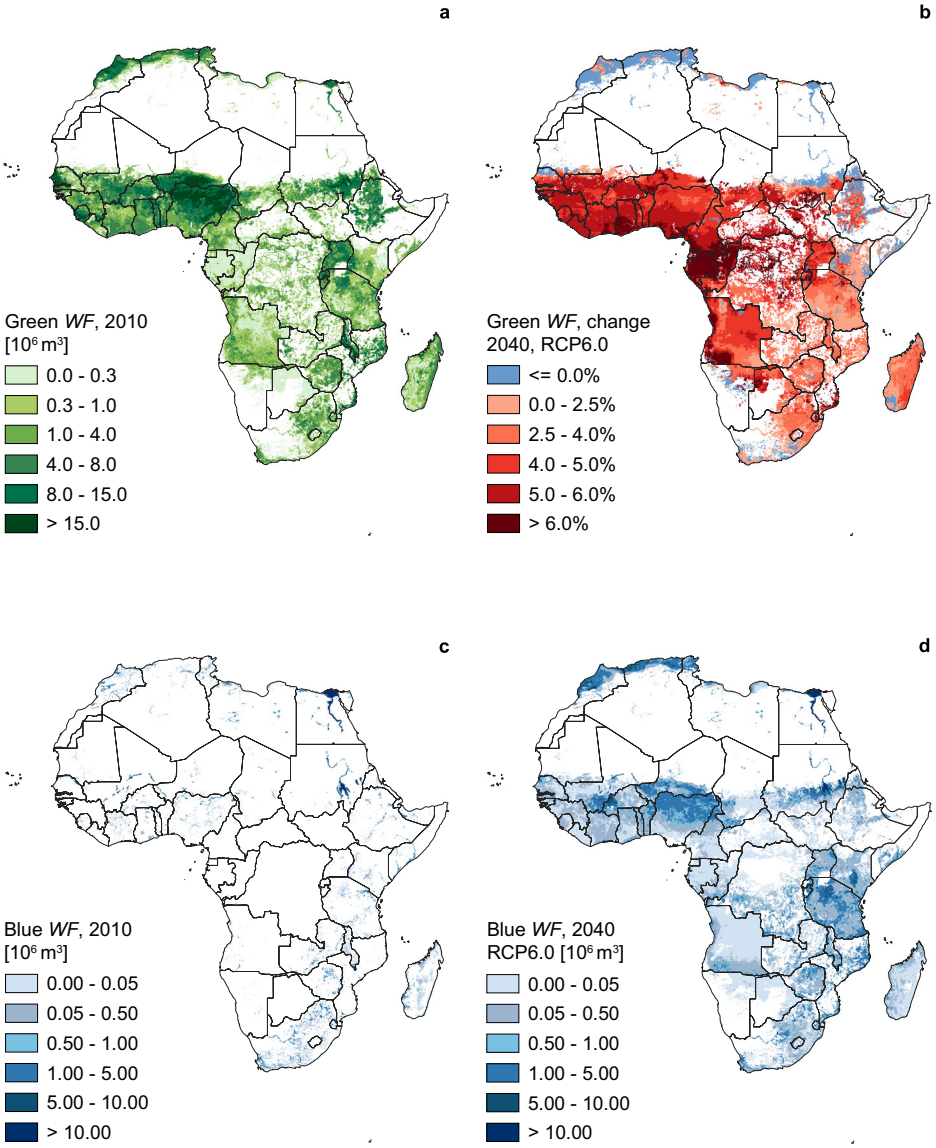

Fig. 1 The water footprint of African agriculture. a Green water footprint of crop production in 2010; (**b**) variation of green water footprint in 2040, RCP6.0 with respect to the year 2010; (**c**) blue water footprint of crop production in 2010; (**d**) blue water footprint of crop production in 2040, RCP6.0, when irrigation is extended to all rainfed areas.

reduced ET_a, since soil moisture availability is limited and cannot meet the growing green water demand. This suggests the occurrence of a drying trend, where cropland will experience increased water stress. Figure 1d displays the blue WF of African agriculture by 2040, RCP 6.0, when, according to our hard-intensification pathway, irrigation infrastructure is expanded over all rainfed areas and advanced management practices are adopted to sustain yield growth, driving a widespread rise in African blue water footprint. We quantify 82.9 Km^3 of additional blue WF for this scenario, with respect to 2010, of which Tanzania accounts for the largest share with a volume of 12.5 Km^3. The total African blue WF further grows in 2070 and reaches 135.5 Km^3 in 2100 (Supplementary Figs. 2, 3). The additional irrigation requirements on rainfed areas are computed as the difference between ET_c and ET_a[23] and are thus higher where this gap is wider, predominantly in the Sahel strip and North Africa.

Repercussions of a hard-intensification scenario on crop unitary water footprint. The uWF indicator dependence on crop yield leads to one of the most evident consequences of the Hard-intensification pathway simulated in this work: a large decrease in total water use intensity by 2040. The Hard-intensification pathway is built on the assumption of an agricultural system which is mainly market-oriented, fully mechanized and which employs optimal irrigation - extended to all rainfed areas -, high yielding varieties, nutrients and chemical pest, disease and weed control application[34]. The steep increase in crop yields achieved by 2040 entails conspicuous reductions in the green uWF of each crop, as shown in Fig. 2, while the blue share of most crops rises, as a consequence of the additional irrigation requirements needed to support the yield growth. Cotton records the highest green water requirement among the crops - $1.13 \cdot 10^4$ m^3 ton^{-1} in 2010 - and the largest increment in blue uWF by 2040, RCP6.0: $3.7 \cdot 10^3$ m^3 ton^{-1}. On the other hand sorghum is the crop exhibiting the largest reduction in green uWF of 83.1% by 2040, RCP6.0. After 2040, management conditions and irrigated areas extension are kept constant in our analysis and the role of climate change becomes more evident in the CWF scenarios. This is visible in Fig. 2, where the uWF of most crops increases after 2040 and the

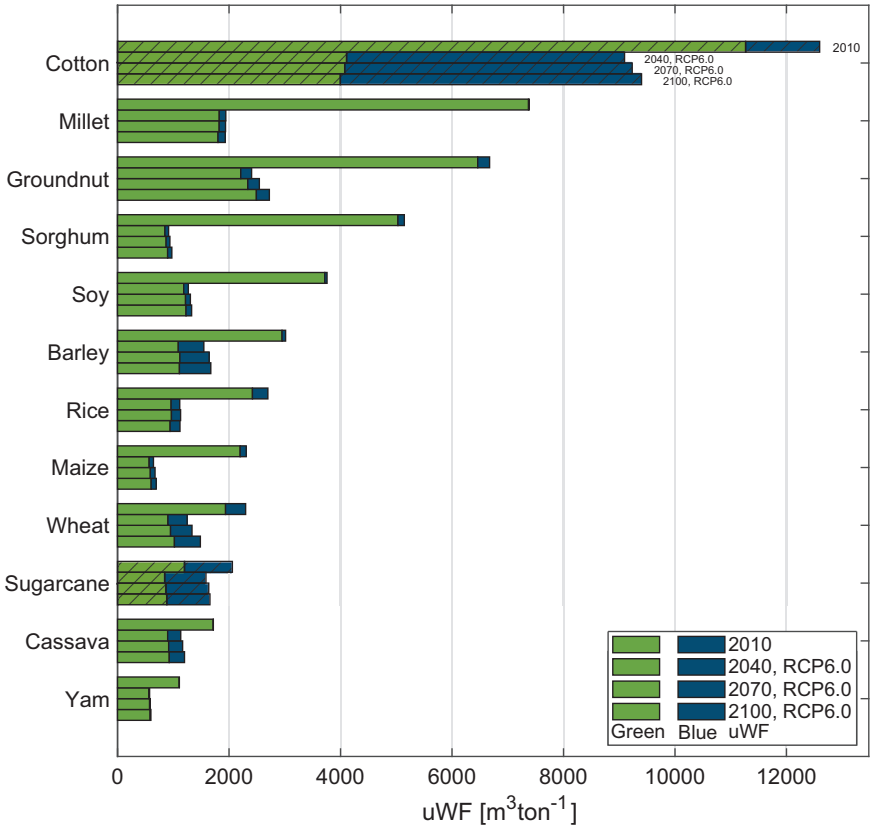

Fig. 2 African average green and blue water footprint per unit weight. Bars show the unit water footprint (uWF) for scenarios 2010, 2040, 2070 and 2100 under the RCP6.0. Colors represent the blue and the green uWF; hatched bars refer to the cash crops.

gap between RCP2.6 and RCP6.0 widens (Supplementary Fig. 6). Rising temperature and ET_c drive green uWF increases in areas where soil moisture availability is sufficient to satisfy higher green water requirements. Where soil moisture is a limiting factor, crop green uWF decreases but the blue water demand grows accordingly to sustain crop yields. Notably, the highest amount of irrigation water, in 2010 as well as in future scenarios, is consumed by cash crops (hatched bars in Fig. 2). Cash crops are mainly grown for their economic value on national and international markets and the water used for their cultivation neither contributes to food security on the continent nor is reflected in their market value[37]. Conversely, as can be observed in Fig. 2, the share of staple crops blue uWF is much lower than the green one, which, excluding areas where rainfall is sufficient to support crop production, highlights a widespread lack of irrigation infrastructures across Africa and a heavy dependence of agriculture on green water[38]. Indeed, only few locations manage to exploit surface and groundwater bodies for irrigation purposes, mostly located in the north and, specifically, along the Nile River[38]. Consequently, in many locations the actual crop yield currently falls below its potential.

Implications of climate change and agricultural intensification for food security. Most of African agriculture relies upon rainfall along the cropping period, thus farmers are exposed to climate variability and extreme events, which impact food security and compromise price stability[38]. Through the average water stress (k_s) condition (see Materials and methods), we highlight how soil moisture is affected by P and ET_a variations in the long term. Such indicator represents the available soil water content in the root zone and it can assume values between 0 (maximum water stress) and 1 (no water stress). Figure 3 shows k_s conditions in 2010 and its changes in 2040, RCP6.0 (see Supplementary Fig. 7 for RCP2.6) over rainfed cropland, where blue areas indicate locations where wetter conditions are expected, as in large parts of Gabon and Uganda. Panel c shows the average k_s change by country in 2040, RCP6.0, ordered by the prevalence of moderate to severe food insecurity in 2019[39] in the population- an indicator measuring the exposition to low quality diets or the lack of food access[39]- and sized proportionately to the extension of each country's rainfed harvested areas. Most of the countries showing a negative average k_s change below 3% are located in Northern Africa, highlighting more arid conditions are to be expected in the coming decades. Nevertheless, North African countries also exhibit a prevalence of food insecurity in the population below the African average (55.6%), since food demand is primarily met through imports rather than national production[40]. Among the most food insecure countries on the Continent, with a prevalence of moderate or severe food insecurity in 80% or above of their population[39], Congo, Somalia, South Sudan, Sierra Leone, and Malawi also exhibits k_s values below the average. Here, insufficient food supply, aggravated by adverse climatic conditions and climate change, is still among the main causes of food insecurity[41]. Figure 4a displays the current distribution of caloric yield on Africa's harvested areas. Most countries record a very low caloric yield in 2010, with Sudan achieving the lowest on the continent ($7.8 \cdot 10^5$ kcal ha^{-1}). Nevertheless, under a hard-intensification scenario, crop yields will drastically improve by 2040, RCP6.0 (see Supplementary Fig. 8 for RCP2.6), boosting food production across the continent, as highlighted in Fig. 4b. Interestingly, the modeled yield growth is unevenly distributed across the continent. Countries showing high prevalence of food insecurity (Fig. 4c), especially the Sahel strip, Central and East African countries, exhibit the largest change, with Lesotho and

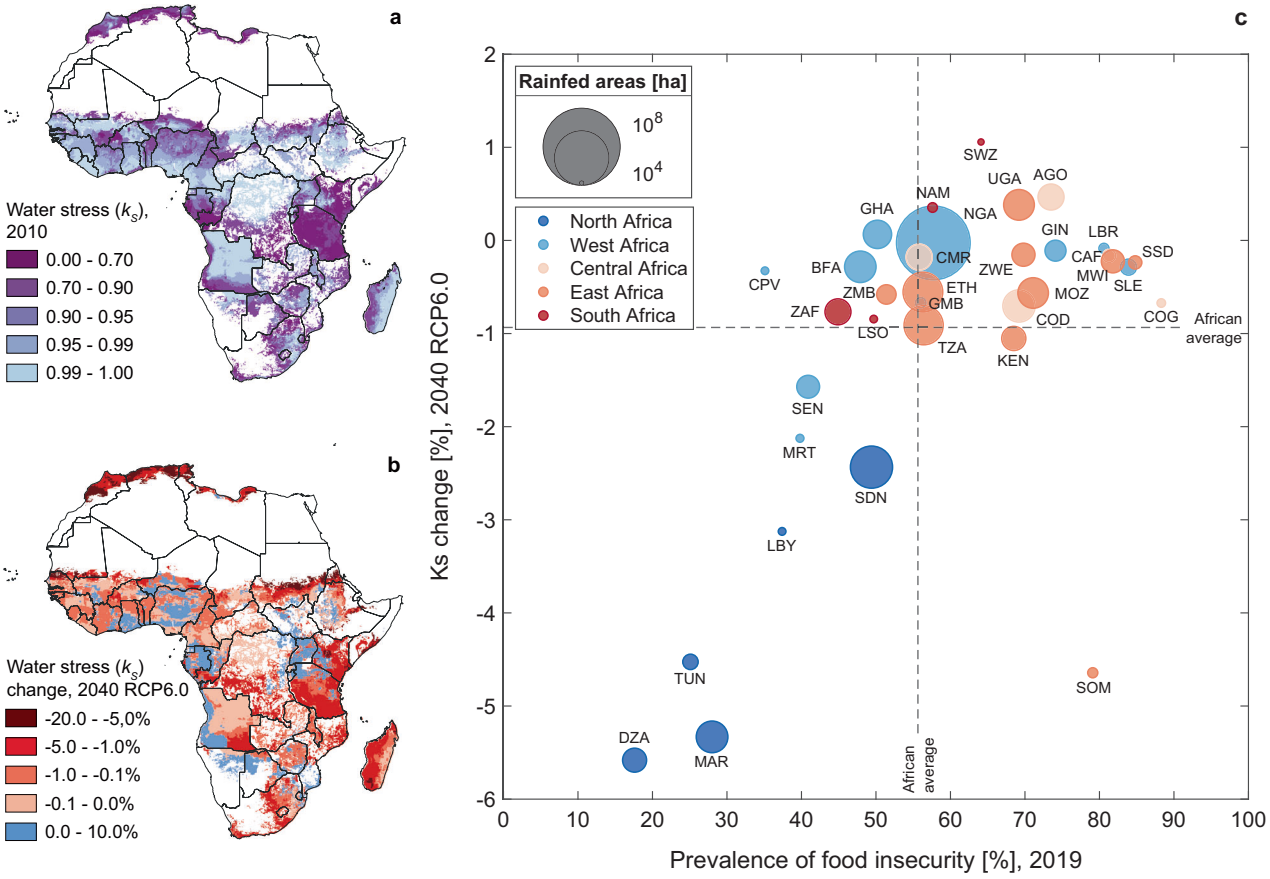

Fig. 3 The impact of climate change on soil moisture availability and the implication for food security. a Average water stress condition in 2010 expressed by the water stress coefficient (k_s); (**b**) variation of the average water stress coefficient by 2040, RCP6.0 compared to 2010; (**c**) country-average variation of water stress coefficient in 2040, RCP6.0, plotted against the prevalence of moderate or severe food insecurity in the population in 2019[39] (refer to Supplementary Table 1 for the complete country name associated to each code). The size of the bubble is proportional to the national rainfed harvested area and the color indicates the region.

Zimbabwe recording a striking variation around 1000%. Such result suggests how food production is the furthest to meet its potential in these countries and suggests that there lies greater potential towards the closure of the yield gap[12].

Testing the reliability of hard-intensification over current extensification trends. The assumptions of constant harvested areas and attainable yield gap closure are very optimistic as they may drive a substantial increase of the African production without causing further agricultural expansion and land clearing over natural areas. We test the reliability of the Hard-intensification pathway over current extensification trends, in order to set our results in perspective with the present situation, by building an Extensification pathway based on data records. We extrapolate the harvested areas expansion in 2040 from extensification trends of areas expansion data ranging from 2000 to 2020[39]. We assume that the same total crop production as in the hard-intensification scenario is achieved and, thus, we derive yield values relative to the extensification scenario from areas and production data. Figure 5 shows the comparison between the two agricultural management scenarios, computed for RCP2.6 and RCP6.0 until 2100. The shaded area located between the intensification scenario (below) and the extensification one (above) highlights the range of variation for WF (Fig. 5a, c, e) and uWF (Fig. 5b, d, f). The extensification trends identified match closely historical data series obtained from Tuninetti et al.[42], suggesting that extensification has been the prevailing management strategy in Africa: 79% of the gross harvested area gain occurred between 2003 and 2019 has been achieved by conversion of primary vegetation to cropland[43]. The coexistence of historical data series[42] and our scenarios between 2010 and 2019 in Fig. 5, provides a validation of the scenarios developed in this study, by anchoring them to the present; divergences between the series are attributable to different data sets employed (see "Material and Methods"). By expanding the harvested area, agricultural extensification employs larger water volumes as production is characterized by lower water use intensity. Indeed, for some crops, such as cassava and rice, the gap between extensification and intensification WF is wide and, as well as for soy, their uWF trends diverge, increasing in the case of extensification and decreasing with intensification. Such result shows an improvement in the water use intensity of these crops for the intensification scenario, but a worsening is expected in the case of extensification, where uWF increases. However, some crops, such as wheat and millet, display a thin shaded area, suggesting that the yield gap and, thus, the area expansion and the water volume needed to achieve their attainable production are small. In addition, crops such as Millet and Sorghum show an impressive reduction of uWF, caused by the assumed yield increase, which, no matter the management scenario, would benefit their water use intensity.

Conclusions

Among the multiple causes for food insecurity in African countries lies insufficient food supply, often provoked by adverse

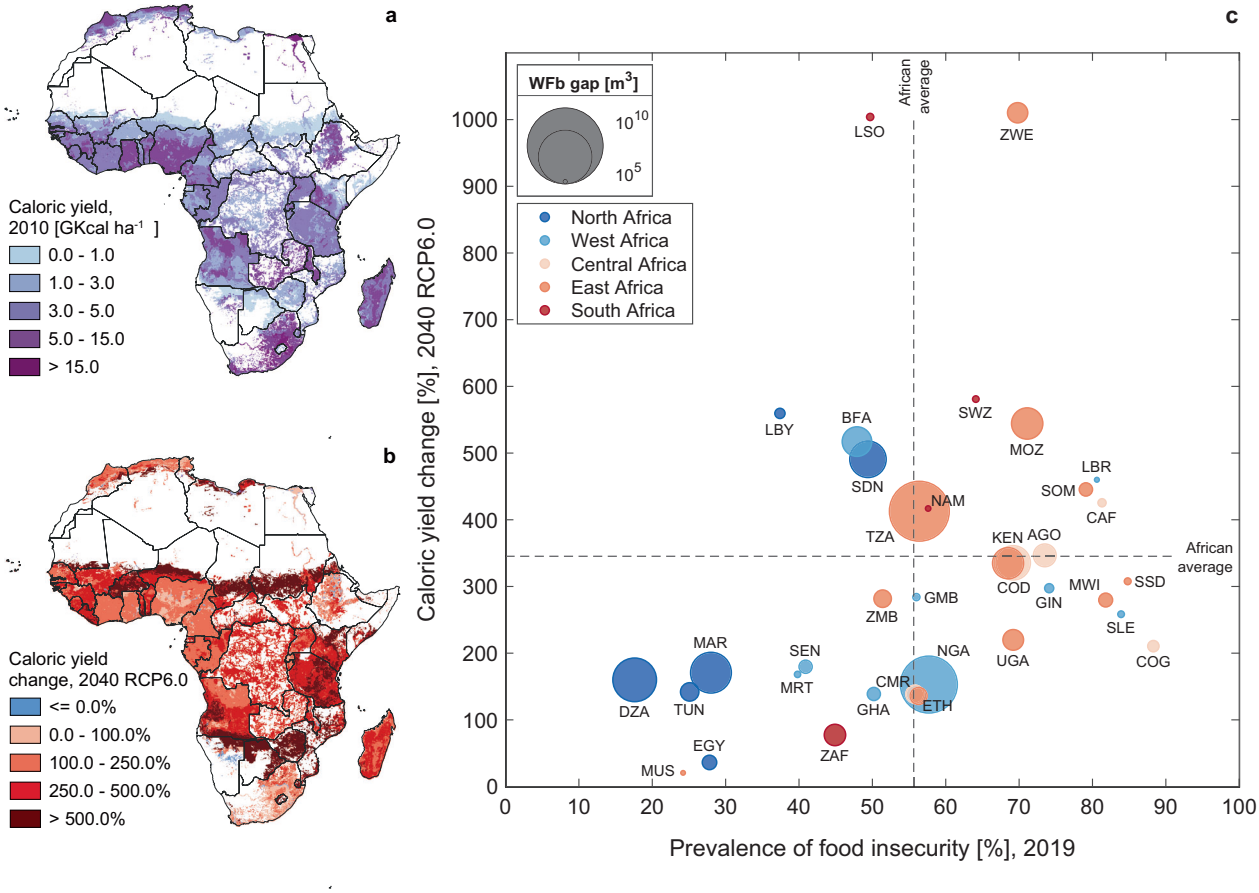

Fig. 4 The impact of climate change on African caloric production. a Caloric yield in 2010; (**b**) caloric yield variation by 2040, RCP6.0 compared to 2010; (**c**) country-average variation of caloric yield in 2040, RCP6.0, plotted against the prevalence of moderate or severe food insecurity in the population in 2019[39] (refer to Supplementary Table 1 for the complete country name associated to each code). The size of the bubble is proportional to the additional m^3 of blue WF caused by the expansion of irrigation; the color indicates the region.

climatic conditions, which can be further aggravated by climate change[41]. We observe changing patterns of P, ET_0 and soil moisture, which might undermine local conditions for agriculture. Recent evidence suggests that crop yields will decrease under future climate conditions[3]; in low-latitudes regions especially, where even moderate temperature increases will negatively impact crop yields due to the current proximity to crop-limiting temperature thresholds for suitable production[1,5]. Furthermore, temperature increases can lead to shortening of growing periods and greater evaporative demand, while CO_2 fertilization effect cannot compensate for such impacts[5]. Improved agricultural management could, therefore, represent a reliable strategy to strengthen food security and for adapting to the negative impacts of climate change. Higher yields and more efficient water use can contribute to reducing the vulnerability of the African agricultural system. The scenario-based analysis performed in this study provides insights into a possible future where African agriculture is fully intensified. Our intent is not to recommend a hard-intensification process over African cropland, but to anticipate some of its consequences, especially those related to sustainable water resources management. We aim to give a critical perspective from the water footprint side to address the commonly adopted strategy of intensification. Agricultural intensification is a main driver of 'planetary boundaries' transgression[1] and the pledge of yield increase comes at an environmental and social cost. High inputs of agro-chemicals leach into soils and water bodies and threaten species living on cropland and in surrounding habitats[44]. By promoting maximized production and a shift toward monoculture, agricultural intensification may eliminate redundancy and diversity within agroecosystems, drive habitat homogenisation and make agriculture more vulnerable to droughts, pests and other shocks[7,44]. In addition, the investments in modern technology might force a transition from smallholder farming to large-scale commercial agriculture[7], marginalizing rural communities, and harming livelihoods and local traditions. Semiarid regions where crops are mainly cultivated under rainfed conditions, typically show the greatest yield increase when irrigation water is supplied[4]. Therefore, the expansion of irrigation infrastructure, supported by a sustainable water management represents a fundamental step towards the strengthening of food security across the continent[45], in the context of a changing climate. Slowing the increase in agricultural water use is of primary importance[1,7] and any strategy aimed at this should integrate food security, socio-economic and environmental well-being, not disregarding locally available technologies, knowledge and rural livelihoods.

The water footprint scenarios developed in this study have been used to assess (i) the implications of an hard-intensification scenario for blue water and green water; (ii) the impact of climate change on green and blue water demand, through crop-specific evapotranspiration scenarios, which shed light on the impact of temperature trends and rainfall variability on soil moisture and on additional irrigation requirements; (iii) the potential of yield intensification to support the improvement of food security, within a water-food nexus framework. The main limitation of this framework is related to the data currently available from the ISI-

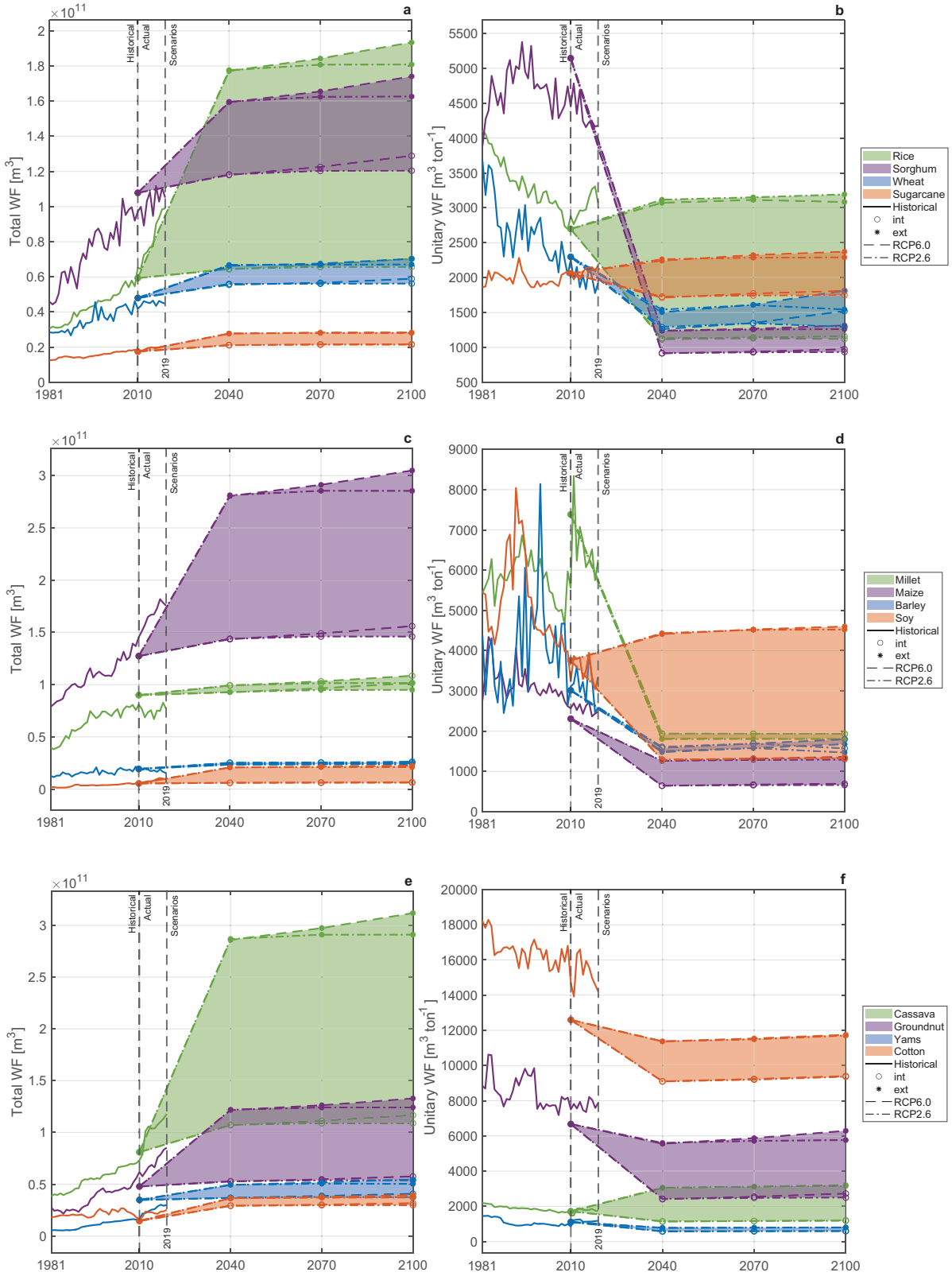

Fig. 5 Historical and future trends of African water footprint. Time-series of total water footprint (WF) and unitary water footprint (uWF) for the 12 study crops: (**a**, **b**) rice, sorghum, wheat, and sugarcane; (**c**, **d**) millet, maize, barley, and soy; (**e**, **f**) cassava, groundnut, yams, and cotton. Solid lines represent historical trends[36,42], dashed and dash-dotted indicate RCP6.0 and RCP2.6, respectively. Empty dots indicate the hard-intensification pathway, stars indicate Extensification pathway. Shaded areas identify the difference in terms of water use of hard intensification and extensification.

MIP round 2b simulations and the GAEZ scenarios, which consider as baseline year 2006 and 2010, respectively, and do not yet integrate SSP-RCP combined scenarios[2]. Future studies on water footprint scenarios should implement the new round (3) of ISI-MIP simulation that is updating the baseline year to 2015, the up-to-date Global Climate Models and the SSP-RCP forcings to better combine climate variables with yields projections. Future studies might expand the water-food nexus analysis to include the quantification of the additional energy demand for water withdrawals to sustain the increased production of high-input agriculture[46]. Scenarios of agricultural land expansions could be explored on a sub-national scale, where also crop-substitution might be analysed as a strategy to maximize production while limiting water[12] and energy demand. The role of international trade in meeting the future food demand in Africa could be examined as well, especially in light of the African Continental Free Trade Area (AfCFTA), which will have implications for the intra-African bilateral trade and, thus, for its future production hubs and their climate vulnerabilities. While further investigation is needed to account for these factors, our findings provide valuable insights for identifying locations where each crop tends to be subject to high climate impacts and where crop production shows trade-offs between high-input management and intensive irrigation demand, thus supporting policymakers and stakeholders.

Materials and methods

Future climatic data pre-elaboration and anchoring to reference climatic observations. We develop forecasts of WF and uWF for twelve major food crops grown in Africa: barley, cassava, cotton, groundnut, maize, millet, rice, sorghum, soybean, sugarcane, wheat and yam. These crops account for 61% of the African crop production (kcal capita^{-1} day^{-1}) and 62% of African harvested area (ha). Climatic data on precipitation (P) and reference potential evapotranspiration (ET_0) are required as input variables for WaterCROP model[24], which is used here to develop water footprint scenarios. We used data records for the period 1961–1990 and climatic model projections of P and ET_0, under baseline conditions with historical and future (RCP2.6 and RCP6.0) climate forcings. P data records for the period 1961–1990 were obtained directly from the University of East Anglia's Climate Research unit (CRU CL v. 2.0)[47] as long-term monthly average gridded data at 10×10 arc min resolution. ET_0 data records for 1961–1990 were provided for the same period by the Food and Agriculture Organization of the United Nations (FAO)[48], which computes evapotranspiration according to the Penman - Monteith method[49], using climatic variables from CRU CL v. 2.0[47], as 5×5 arc min resolution monthly long-term averages. Historical model projections for the periods 1961–1990 and 1981–2005, and future climate projections ranging from 2011 to 2100 of monthly P and ET_0 were sourced from the ISI-MIP repository - simulation round ISI-MIP2b[50] as 30×30 arc min gridded data. Specifically, monthly ET_0 projections were provided as the output of PCR-GLOBWB global hydrological model[51], driven by four different Global Climate Models (GCMs) - GFDL-ESM2M, HadGEM2-ES, IPSL-CM5A-LR, MIROC5 - as climate forcings, while monthly P projections at 30×30 arc min resolution were obtained from the same four different GCMs as ISI-MIP input data. Both ET_0 and P data sets were downscaled to 5×5 arc min and long-term monthly averages were performed over five thirty-years intervals: 1961–1990 (data records and historical climate projections), 1981–2005 (baseline interval; ISI-MIP historical forcing ends in year 2005, therefore, to be consistent, the period used to build the 2010 present scenario spans the years from 1981 to 2005), 2011–2040, 2041–2070, 2071–2100. Intervals covering future time periods were simulated under both RCP2.6 and RCP6.0 - available for all simulation periods and GCMs; the choice of the RCPs included depends on the availability of the ISI-MIP climatic projections. In order to prepare the climatic variables describing each scenario for which results are presented, we calculated the difference between each present (1981–2005) or future (2011–2100) projection time interval of P and ET_0 and ISI-MIP2b model projections relative to the period 1961–1990. Then, the anomaly obtained in this way was added to the reference P[47] and ET_0[48] data records for 1961–1990. The practice of adding the perturbation - consisting in the difference between the modeled future climate projection and the historical climate simulation - to an observed reference climate is a standard in the analysis of climate model results[45], since, by 'anchoring' the modeled climate change to a commonly observed reference, greater confidence can be attributed to the results. This is necessary since historical climate simulations differ among models, which also vary in their assumptions and in the representation of some processes[5].

Crop-specific properties and agricultural management practices. Spatially distributed (5 arc minute; 1/12°; ~ 10 km), crop-specific information on rainfed and irrigated yields (ton ha^{-1}) and harvested areas (ha) were sourced from the Global - Agro Ecological Zones (GAEZ v4) database. The AEZ methodology estimates potential yields for historical, current and future climatic conditions, the last of which are simulated by five GCMs - GFDL-ESM2M, HadGEM2-ES, IPSL-CM5A-LR, MIROC-ESM-CHEM, NorESM1-M - and four RCPs[34]. Potential yield is a constraint-free yield which represents the agronomically possible upper limit of crop production with regard to temperature and radiation regimes prevailing in each grid-cell[34]. Yield reduction factors such as temperature and frost hazards, climatic factors affecting farming operations, damages caused by pests, diseases and weeds on plant growth and on the quality of the product are computed and combined with agro-climatic potential yields and constraints induced by soil limitations and terrain-slope conditions. Thus, GAEZ v4 estimates agro-ecological attainable yields, which we used to calculate the uWF (m^3 ton^{-1}). The attainable yield values are available as averaged over thirty-years intervals, of which we used 2011–2040, 2041–2070 and 2071–2100 under RCPs 2.6 and 6.0. The future yield projections employed in this work include assumptions about future CO_2 concentration in the atmosphere and its fertilization effect on plant growth. In addition, GAEZ v4 provides a spatial representation of current actual yields and harvested areas for year 2010, obtained by downscaling the annual national average of 2009–2011 FAOSTAT[39] statistics to individual spatial units (grid cells)[34]. We used actual yield values in 2010 for the baseline scenario, instead of historical simulations over 1981–2010. The harvested areas data set refers to year 2010 and is used in each scenario as a time-independent variable, in order to simulate a form of agricultural intensification over the continent. While GAEZ provides actual statistics as fresh/harvest weight, attainable yields are available as dry weight for most crops, as sugar weight for sugar cane or as lint weight for cotton. Therefore, conversion factors, as indicated in the model documentation[34], have been applied to convert actual statistics, relative to the 2010 scenario, to dry weight. The conversion coefficients depend on the moisture content of harvested products and, in some cases such as sugar crops, are derived from technical extraction rates[34]. The same procedure was applied to FAOSTAT crop statistics as they are provided at fresh weight. The MIRCA2000[52] data set was adopted for growing period lengths, sowing and harvesting dates; however, a discrepancy was observed between the spatial coverage of this data set and the

crops' harvested areas extension in 2010. Therefore, an interpolation process was performed to extend planting dates and growing period information to the coverage of GAEZ harvested areas data set. Crop coefficients, soil properties, soil available water content, root zone depth and the depletion fraction were derived from a previous study[24].

Future scenarios of crop water footprint. To compute the water footprint of every crop for each scenario, the high-resolution crop water footprint model WaterCROP[24] was used. It evaluates the WF of multiple crops at the spatial resolution of 5 × 5 arc min, distinguishing between rainfed and irrigated production conditions. Some relevant modifications were brought to the model, incorporating important updates in the temporal resolution of input data, for it to provide outputs at monthly resolution, thereby improving WaterCROP temporal resolution, and implementing the future time dimension, in order to develop future water footprint scenarios.

WaterCROP performs spatially-explicit estimates of daily crop-specific actual evapotranspiration $ET_{a,j}$ (where j runs from the planting day to the harvesting day), which quantifies the amount of water (in mm day^{-1}) that a crop consumes via evapotranspiration throughout the growing season. This is a function of climatic and phenological properties, as well as agricultural practices[24]. WaterCROP determines daily ET_0 through a linear interpolation of monthly ET_0 data[47,50], with monthly averages assigned to the middle of each month. Daily $ET_{a,j}$ is then calculated following the FAO56 method[49] for each year. The $ET_{a,j}$ estimate is equal to the product of: the daily water stress coefficient ($k_{s,j}$), that is a proxy for the daily water deficiency in the unsaturated soil layer; the daily crop coefficient ($k_{c,j}$), that integrates the effects of crop height, crop-soil surface resistance, and albedo of the crop-soil surface; and the daily ET_0 from a hypothetical well-watered grass surface with fixed crop height, albedo and canopy resistance[24]. Thus, the daily $ET_{a,j}$ reads:

$$ET_{a,j} = k_{s,j} \cdot k_{c,j} \cdot ET_{0,j}. \quad (1)$$

The estimate of $k_{s,j}$ in each grid cell varies daily depending on the total available water content (TAWC), the readily available water content in the root zone (RAWC), where RAWC is the portion of TAWC that the crop can actually use[49], and the crop-specific rooting depth[24]. For rainfed production, WaterCROP computes the water stress coefficient through a daily steady-state water balance[24]. In this case, every time water from precipitation is not sufficient for optimal evapotranspiration (i.e., $ET_{c,j} = k_{c,j} \cdot ET_{0,j}$), the crop becomes stressed and the water stress coefficient drops below 1. For irrigated production, the model assumes that the crop receives all the water required to optimally evapotranspire via irrigation, even when water is not available from precipitation. Hence, the water stress coefficient is equal to 1 throughout the growing period[24]. Taking the sum of the daily $ET_{a,j}$ values for the entire growing season gave the annual ET_a estimate for a crop in a grid cell. Therefore, annual ET_a is evaluated over the different time interval and for each study crop, thus providing one present (2010) and three future scenarios (2040, 2070, 2100; for RCP2.6 and RCP6.0) of crop water requirement, available for further agri-hydrological analyses.

WaterCROP computes the green ($ET^R_{a,g}$ and $ET^I_{a,g}$) and blue ($ET^I_{a,b}$) shares of the crop actual evapotranspiration over the growing period, in order to evaluate the distinct contributions of precipitation (green) and irrigation (blue) water to the crop water footprint. The model calculates the total P along the growing period, for irrigated and rainfed production, and the effective P, which includes only the component of P which is used by the plants and it is not lost as runoff[24]. The crop water footprint is provided as disaggregated in its green (uWF_g), blue (uWF_b), rainfed (uWF_{rf}), irrigated (uWF_{irr}) components and it is evaluated both in volume (m^3) (WF) and per unit of production (m^3 ton^{-1}) (uWF). The computation of rainfed and irrigated production water footprint represents a further innovation introduced in the WaterCROP tool. Specifically, the rainfed production only includes the rainfed share of the green crop actual evapotranspiration over the growing period and the rainfed crop yield (Y_{rf}), while the irrigated production includes blue and green water evapotranspired by the crop and the irrigated crop yield (Y_{irr}). The computation of each uWF component is the following:

$$uWF_{rf} = \frac{10 \cdot ET^R_{a,g}}{Y_{rf}} \left(\frac{m^3}{ton}\right) \quad (2)$$

$$uWF_{irr} = \frac{10 \cdot (ET^I_{a,b} + ET^I_{a,g})}{Y_{irr}} \left(\frac{m^3}{ton}\right) \quad (3)$$

$$uWF_{g} = \frac{10 \cdot (ET^R_{a,g} + ET^I_{a,g})}{Y_{tot}} \left(\frac{m^3}{ton}\right) \quad (4)$$

$$uWF_{b} = \frac{10 \cdot ET^I_{a,b}}{Y_{tot}} \left(\frac{m^3}{ton}\right) \quad (5)$$

Uncertainty analysis. The scenario-based analysis performed in this work is based on projections of the main CWF components: ET_0, P (climate related) and yields (technology and climate related). Hence, we acknowledge different sources of uncertainty. The first source is related to the uWF estimates, for which the uncertainty is relatively low[42]. In particular, we acknowledge an error in the uWF estimates due to model assumptions of 9.3% for wheat, 10% for rice and maize, and 13% for soybean of 13% ([42,53]). The uncertainty related to the evapotranspiration estimates is relatively low especially when $ET_a = ET_c$ because in this case it is mostly driven by the uncertainty in ET_0. The estimates of evapotranspiration depend on a number of key parameters (e.g., planting date, available water content, length of the growing period). It has been shown that wheat is the most sensitive crop to the length of the growing period, rice to the reference evapotranspiration, maize and soybean to the crop planting date[54]. Moreover, the estimates are also sensitive to the model adopted to evaluate the reference evapotranspiration. However, Rolle et al. 2021[55] has shown that the monthly ET_0 obtained with the Penman Monteith method (from the CRU-TS v.4) well compare with those obtained from the ERA5-based Hargreaves-Samani method (Pearson coefficient of 0.99), thus well supporting the adoption of the Penman Monteith estimates as recommended by the FAO56 methodology[49,56]. Finally, the uncertainty related to yield projections is expected to be the largest one, since yield scenarios depend, among all, on socio-economic development whose uncertainty cannot be quantified here, nor it is communicated by GAEZ v4 that we used as a source of yield projection.

Markers of water stress and food insecurity. In an effort to disentangle the breadth of meaning that the CWF indicator encompasses, we developed two indicators of, respectively, soil water stress and agricultural caloric production on the African continent. The former is the average water stress condition (k_s), which is the average daily water stress coefficient along the growing season of rainfed agriculture. It depends on the available soil water content in the root zone and it assumes values between 0 (maximum water stress) and 1 (no water stress). k_s was computed for each scenario, for each crop and in its aggregated form

over the twelve crops included in the study. It was computed as follows:

$$k_s = \frac{\sum_{\delta=1}^{LGP} ET_{a,j}^{R}}{\sum_{\delta=1}^{LGP} ET_{c,j}^{R}} \quad (6)$$

where $ET_{c,j}$ is the maximum attainable evapotranspiration when $k_{s,j}$ equals 1[24].

The latter indicator of caloric production is the caloric yield. Crop yields were expressed in (kcal ha^{-1}) through the conversion factors provided by USDA - Food Composition Database[57]. Then, a weighted average was performed over the harvested areas; only staple crops were included in the calculation, since cash crops do not contribute with calories to food security.

Both indicators were compared with the prevalence of moderate or severe food insecurity for the year 2019 (provided by FAOSTAT as a three-year average over the period 2018-2020), an indicator for the exposition to low quality diets or lack of food access[39]. The prevalence of moderate or severe food insecurity is an estimate of the percentage of people in the population who inhabit households classified as moderately or severely food insecure. This classification is given when at least one adult in the household has been exposed to low quality diets and might have been forced to reduce the amount of food normally consumed because of a lack of money or other resources[39].

Crop model description and agricultural pathways preparation. Crop yields data have been sourced from GAEZ v4[34], as mentioned above, because the dataset guarantees the availability of actual (2010) crop data, which allow the anchoring of simulations to present conditions, as well as for its high-input assumption on future attainable yields, as explained below. GAEZ v4 integrates the Agro-Ecological Zones (AEZ) methodology[34], used to assess natural resources for identifying suitable agricultural land utilization options, as well as a comprehensive global database for the characterization of climate, soil and terrain conditions relevant to agricultural production. It provides fundamental information on the current and future state of agriculture, on its irrigation demand, development opportunities, risks and adaptation options[34]. The AEZ methodology most relevant feature for this work is the attribution to all future simulations of advanced agricultural management practices with high inputs levels. GAEZ v4 describes an agricultural system which, by 2040, is mainly market oriented, fully mechanized and which employs optimal irrigation with full and adequate artificial drainage systems, high yielding varieties, nutrients and chemical pest, disease and weed control application[34]. Accordingly, we have adapted our methodology to include the non-linear linkage between crop yield and crop water use to obtain water footprint results mirroring the GAEZ attainable crop yields. According to the GAEZ documentation[34], we combine the Hard-intensification pathway with optimal irrigation practices to avoid crop water stress and guarantee optimal soil moisture throughout the growing season. Hence, in order to achieve the projected attainable yields over currently rainfed areas - in addition to high inputs of fertilizers, nutrients and chemical pest, disease and weed control application assumed by the AEZ methodology - we assume that, by 2040 (first interval for which GAEZ provides attainable yields), irrigation infrastructure is expanded to all currently rainfed areas to meet the increased crop water demand. We quantify the additional blue water needed to support the yield growth projected by GAEZ and the related additional blue water footprint by calculating the difference between the crop potential evapotranspiration (ET_c - now associated with maximum attainable yields) and the crop actual evapotranspiration (ET_a - associated with current yields) on rainfed harvested areas. This difference represents the amount of blue water that needs to be provided through irrigation to increase actual yields to their maximum attainable value[23].

Crop yield increase, irrigated areas expansion over rainfed areas and fixed total harvested areas until 2100 constitutes the core assumptions of the Hard-intensification pathway we developed. This aligns with the shared socio-economic pathway (SSP) SSP 5, which prospects a future where resource-intensive land management drives a rapid increase in crop yields[35]. Nonetheless, our Hard-intensification pathway differs from SSP 5 in the representation of land use change, since we assume no future cropland expansion, in order to focus only on agricultural intensification effects on water resources. Furthermore, the Extensification pathway we discuss in this work is coherent with SSP 2, which describes a world in which social, economic, and technological trends do not shift markedly from historical patterns. In this context, land use change is incompletely regulated, deforestation and land clearance continue at slowly declining rates over time, rates of crop yield growth decline slowly over time, but low-income regions catch up with high-income countries to a certain extent[35]. In addition, the climatic description is performed through the inclusion of the RCP 2.6 and RCP 6.0 in the future projections - which were chosen in order to be consistent with ISI-MIP climatic variables ET_0 and P.

Each water footprint scenario is the result of long term averages spanning over thirty years for the intervals 1981–2010, 2011–2040, 2041–2070, 2071–2100, in order to remove the input data dependency of interannual fluctuations. The subdivision in 30-years intervals was guided by GAEZ v4 yield data set organization, it was therefore applied to climatic variables data and ultimately reflected in the water footprint scenarios. Regarding climatic and yield data estimates, we use the ensemble obtained as the average of all the GCMs realizations available. Harvested areas have been kept constant at 2010 extension for each spatially distributed scenario. Additionally, current cropland extensification trends were computed from FAOSTAT[39] harvested areas extension data for each crop, ranging from 2000 to 2020, and extrapolated until 2040. These were used to scale continent-aggregated values of WF and uWF, in Fig. 5, according to current extensification trends, while assuming the same total crop production as the hard-intensification scenario is achieved. The co-presence of present yearly calculations[42] and our estimates between 2010 and 2019 in Fig. 5 constitutes a validation of the scenarios developed in this study. The trends identified are coherent with historical data records, which validates our forecasts and allow to anchor the scenarios developed to the present. Divergences between the series are attributable to the different data sets employed in the studies[42].

Data availability

All the input data used in this study are from publicly available sources. Climate data projections of ET_0 and P are available from the ISI-MIP repository - simulation round ISI-MIP2b (https://data.isimip.org/search/tree/ISIMIP2b%252FOutputData%252Fagriculture/). P observations are available from from the University of East Anglia's Climate Research unit (CRU CL v. 2.0; https://crudata.uea.ac.uk/cru/data/hrg/tmc/). ET_0 observations are distributed by the Food and Agriculture Organization of the United Nations (FAO) at https://data.apps.fao.org/map/catalog/srv/eng/catalog.search#/metadata/db326f70-88fd-11da-a88f-000d939bc5d8. Crop-specific information on rainfed and irrigated yields and harvested area are available from the Global - Agro Ecological Zones (GAEZ v4) database (https://gaez.fao.org/). The dataset generated in the current study is available at https://doi.org/10.5281/zenodo.10024627.

Code availability

The codes developed for the analyses and to generate results are available from the corresponding author on request.

Received: 11 January 2023; Accepted: 17 November 2023;
Published online: 13 December 2023

References

1. Jägermeyr, J. et al. Climate impacts on global agriculture emerge earlier in new generation of climate and crop models. *Nat. Food* **2**, 873–885 (2021).
2. IPCC, Climate Change 2021: The Physical Science Basis. Contribution of Working Group I to the Sixth Assessment Report of the Intergovernmental Panel on Climate Change [Masson-Delmotte, Zhai, V., P. et al. (eds.)], Cambridge University Press, Cambridge, United Kingdom and New York, NY, USA, 2391 pp., (2021).
3. Ray, D. K. et al. Climate change has likely already affected global food production. *PLoS ONE* **14**, e0217148 (2019).
4. Elliott, J. et al. Constraints and potentials of future irrigation water availability on agricultural production under climate change. *PNAS* **111**, 3239–3244 (2014).
5. Rosenzweig, C. et al. Assessing agricultural risks of climate change in the 21st century in a global gridded crop model intercomparison. *PNAS* **111**, 3268–3273 (2014).
6. Ray, D. K., Mueller, N. D., West, P. C. & Foley, J. A. Yield trends are insufficient to double global crop production by 2050. *PLoS ONE* **8**, e66428 (2013).
7. Davis, K. F., Rulli, M. C., Seveso, A. & D'Odorico, P. Increased food production and reduced water use through optimized crop distribution. *Nat. Geosci.* **10**, 919–924 (2017).
8. Berkhout, P., Bergevoet, R., van Berkum, S. A brief analysis of the impact of the war in Ukraine on food security, Wageningen Economic Research, Policy Document 2022-033, (2022).
9. FAO, IFAD, UNICEF, WFP, WHO, The State of Food Security and Nutrition in the World 2021. Transforming food systems for food security, improved nutrition and affordable healthy diets for all, FAO, https://doi.org/10.4060/cb4474en (2021).
10. Davis, K. F., D'Odorico, P. & Rulli, M. C. Moderating diets to feed the future. *Earth's Fut.* **2**, 559–565 (2014).
11. Mueller, N. D. et al. Closing yield gaps through nutrient and water management. *Nature* **490**, 254–257 (2012).
12. Davis, K. F. et al. Water limits to closing yield gaps. *Adv. Water Resources* **99**, 67–75 (2017).
13. Bain, L. E. et al. Malnutrition in sub saharan africa: Burden, causes and prospects. *Pan Afr. Med. J.* **15**, 120 (2013).
14. Jemmali, H. Water poverty in africa: A review and synthesis of issues, potentials, and policy implications. *Soc. Indic. Res.* **136**, 335–358 (2018).
15. Porkka, M., Gerten, D., Schaphoff, S., Siebert, S. & Kummu, M. Causes and trends of water scarcity in food production. *Environ. Res. Lett.* **11**, 015001 (2016).
16. Rockström, J. et al. Sustainable intensification of agriculture for human prosperity and global sustainability. *Ambio* **46**, 4–17 (2017).
17. van Ittersum, M. K. et al. Can sub-saharan africa feed itself? *PNAS* **113**, 14964–14969 (2016).
18. Tian, X. & Yu, X. Crop yield gap and yield convergence in african countries. *Food Secur.* **11**, 1305–1319 (2019).
19. Ariga, J., Mabaya, E., Waithaka, M. & Wanzala-Mlobela, M. Can improved agricultural technologies spur a green revolution in africa? a multicountry analysis of seed and fertilizer delivery systems. *Agric. Econ.* **50**, 63–74 (2019).
20. Foley, J. A. et al. Solutions for a cultivated planet. *Nature* **478**, 337–342 (2011).
21. Giller, K. E. The food security conundrum of sub-saharan africa. *Global Food Secur.* **26**, 100431 (2020).
22. Otsuka, K. & Muraoka, R. A green revolution for sub-saharan africa: Past failures and future prospects. *J. African Econ.* **26**, i73–i98 (2017).
23. Siebert, S. & Döll, P. Quantifying blue and green virtual water contents in global crop production as well as potential production losses without irrigation. *J. Hydrol.* **384**, 198–217 (2010).
24. Tuninetti, M., Tamea, S., D'Odorico, P., Laio, F. & Ridolfi, L. Global sensitivity of high-resolution estimates of crop water footprint. *Water Resour. Res.* **51**, 8257–8272 (2015).
25. D'Odorico, P. et al. Global virtual water trade and the hydrological cycle: patterns, drivers, and socio-environmental impacts. *Environ. Res. Lett.* **14**, 053001 (2019).
26. D'Odorico, P. et al. The global food energy water nexus. *Rev. Geophys.* **56**, 456–531 (2018).
27. Mekonnen, M. M. & Hoekstra, A. Y. The green, blue and grey water footprint of crops and derived crop products. *Hydrol. Earth Syst. Sci.* **15**, 1577–1600 (2011).
28. Ercin, A. E. & Hoekstra, A. Y. Water footprint scenarios for 2050: A global analysis. *Environ. Int.* **64**, 71–82 (2014).
29. Garofalo, P. et al. Water footprint of winter wheat under climate change: Trends and uncertainties associated to the ensemble of crop models. *Sci. Total Environ.* **658**, 1186–1208 (2019).
30. Elbeltagi, A. et al. The impact of climate changes on the water footprint of wheat and maize production in the nile delta, egypt. *Sci. Total Environ.* **743**, 140770 (2020).
31. Liu, Y. et al. Enhancing water and land efficiency in agricultural production and trade between central asia and china. *Sci. Total Environ.* **780**, 146584 (2021).
32. Xu, X., Zhang, Y. & Chen, Y. Projecting china's future water footprint under the shared socio-economic pathways. *J. Environ. Manag.* **260**, 110102 (2020).
33. Masud, B. M., McAllister, T., Cordeiro, M. & Faramarzi, M. Modeling future water footprint of barley production in alberta, canada: Implications for water use and yields to 2064. *Sci. Total Environ.* **616**, 208–222 (2018).
34. FAO, IIASA, Global Agro-Ecological Zones (GAEZ v4) - Data Portal user's guide, FAO, (2021).
35. Riahi, K. et al. The shared socioeconomic pathways and their energy, land use, and greenhouse gas emissions implications: An overview. *Global Environ. Change* **42**, 153–168 (2017).
36. Tamea, S., Tuninetti, M., Soligno, I. & Laio, F. Virtual water trade and water footprint of agricultural goods: The 1961–2016 cwasi database. *Earth Syst. Sci. Data* **13**, 2025–2051 (2021).
37. Falsetti, B., Vallino, E., Ridolfi, L. & Laio, F. Is water consumption embedded in crop prices? a global data-driven analysis. *Environ. Res. Lett.* **15**, 104016 (2020).
38. De Angelis, P. et al. Data-driven appraisal of renewable energy potentials for sustainable freshwater production in africa. *Renew. Sustain. Energy Rev.* **149**, 111414 (2021).
39. FAOSTAT, Faostat, [Accessed: September 2021] (2021).
40. Antonelli, M. & Tamea, S. Food-water security and virtual water trade in the middle east and north africa. *Int. J. Water Resources Dev.* **31**, 326–342 (2015).
41. Gebre, G. G. & Rahut, D. B. Prevalence of household food insecurity in east africa: Linking food access with climate vulnerability. *Clim. Risk Manag.* **33**, 100333 (2021).
42. Tuninetti, M., Tamea, S., Laio, F. & Ridolfi, L. A fast track approach to deal with the temporal dimension of crop water footprint. *Environ. Res. Lett.* **12**, 074010 (2017).
43. Potapov, P. et al. Global maps of cropland extent and change show accelerated cropland expansion in the twenty-first century. *Nat. Food* **3**, 19–28 (2022).
44. Zabel, F. et al. Global impacts of future cropland expansion and intensification on agricultural markets and biodiversity. *Nat. Commun.* **10**, 2844 (2019).
45. Rosa, L. et al. Potential for sustainable irrigation expansion in a 3 °c warmer climate. *PNAS* **117**, 29526–29534 (2020).
46. Falchetta, G. et al. A renewable energy-centred research agenda for planning and financing nexus development objectives in rural sub-saharan africa. *Energy Strategy Rev.* **43**, 100922 (2022).
47. New, M., Lister, D., Hulme, M. & Makin, I. A high-resolution data set of surface climate over global land areas. *Clim. Res.* **21**, 1– (2002).
48. FAO, Fao map catalog, [Accessed: November 2021] (2014).
49. Allen, R. G. et al. Crop evapotranspiration-guidelines for computing crop water requirements-fao irrigation and drainage paper 56. *Fao, Rome* **300**, D05109 (1998).
50. Frieler, K. et al. Assessing the impacts of 1.5 °c global warming - simulation protocol of the inter-sectoral impact model intercomparison project (isimip2b). *Geosci. Model Dev.* **10**, 4321–4345 (2017).
51. Sutanudjaja, E. H. et al. Pcr-globwb 2: a 5 arcmin global hydrological and water resources model. *Geosci. Model Dev.* **11**, 2429–2453 (2018).
52. Portmann, F. T., Siebert, S. & Döll, P. Mirca2000-Global monthly irrigated and rainfed crop areas around the year 2000: A new high-resolution data set for agricultural and hydrological modeling. *Global Biogeochem. Cycles* **24**, GB1011 (2010).
53. De Petrillo, E., Tuninetti, M., Ridolfi, L. & Laio, F. International corporations trading brazilian soy are keystone actors for water stewardship. *Commun Earth Environ* **4**, 87 (2023).
54. Tuninetti, M., Tamea, S., D'Odorico, P., Laio, F. & Ridolfi, L. Global sensitivity of high-resolution estimates of crop water footprint. *Water Resources Res.* **51**, 8257–8272 (2015).
55. Rolle, M., Tamea, S. & Claps, P. Climate-driven trends in agricultural water requirement: an era5-based assessment at daily scale over 50 years. *Environ. Res. Lett.* **17**, 044017 (2022).
56. Pereira, L., Paredes, P. & Jovanovic, N. Soil water balance models for determining crop water and irrigation requirements and irrigation scheduling focusing on the fao56 method and the dual kc approach. *Agric. Water Manag.* **241**, 106357 (2020).
57. USDA, Fooddata central, [Accessed: November 2022] (2022).

Author contributions

V.G., M.T. and F.L. designed the study. V.G. and M.T. conducted the analyses and V.G. produced the figures. V.G., M.T. and F.L. contributed to data interpretation. V.G. and M.T. wrote the first draft of the paper. V.G., M.T. and F.L. edited the paper.

Competing interests
The authors declare no competing interests.

Additional information
Supplementary information The online version contains supplementary material available at https://doi.org/10.1038/s43247-023-01125-5.

Correspondence and requests for materials should be addressed to Vittorio Giordano.

Peer review information *Communications Earth & Environment* thanks the anonymous reviewers for their contribution to the peer review of this work. Primary Handling Editors: Jinfeng Chang and Aliénor Lavergne. A peer review file is available.

Reprints and permission information is available at http://www.nature.com/reprints

Publisher's note Springer Nature remains neutral with regard to jurisdictional claims in published maps and institutional affiliations.

Open Access This article is licensed under a Creative Commons Attribution 4.0 International License, which permits use, sharing, adaptation, distribution and reproduction in any medium or format, as long as you give appropriate credit to the original author(s) and the source, provide a link to the Creative Commons license, and indicate if changes were made. The images or other third party material in this article are included in the article's Creative Commons license, unless indicated otherwise in a credit line to the material. If material is not included in the article's Creative Commons license and your intended use is not permitted by statutory regulation or exceeds the permitted use, you will need to obtain permission directly from the copyright holder. To view a copy of this license, visit http://creativecommons.org/licenses/by/4.0/.

© The Author(s) 2023